ANTI-ICING STUDY FOR REFRIGERATED CONTAINER BASED ON VARIOUS HEATING WIRE FORMS

by

Jinfeng WANG [a,b,c*], ***Huanglei ZHU*** [a,b], ***Yuyao SUN*** [a,b], ***and Jing XIE*** [a,b,c,d*]

[a] College of Food Science and Technology, Shanghai Ocean University, Shanghai, China
[b] Shanghai Professional Technology Service Platform on Cold Chain Equipment Performance and Energy Saving Evaluation, Shanghai, China
[c] Shanghai Engineering Research Center of Aquatic Product Processing and Preservation, Shanghai, China
[d] National Experimental Teaching Demonstration Center for Food Science and Engineering, Shanghai Ocean University, Shanghai, China

Original scientific paper
https://doi.org/10.2298/TSCI221013215W

In this paper, the effect of different forms of electric heating wire forms on the anti-icing performance of the refrigerated container was studied based on numerical simulation. The heat transfer and the thermal conductivity of the refrigerated container door wall, and the uniformity of air-flow distribution in the refrigerated container are analyzed. The heating wire form 2 has the best anti-icing performance and meets the anti-icing requirement when the thermal conductivity is from 0.005-0.01 W/mK. The electric heating wires nearest to the inner wall surface is the optimal anti-icing solution. The spare electric heating wires placement can be determined according to the thickness of the refrigerated container door. The specific lay-out of electric heating wires in the future can be further optimized in combination with carbon emissions.

Key words*: anti-icing performance, heating wire, refrigerated container, heat transfer*

Introduction

In order to provide high quality chilled food, the cold chain is widely used now, which can keep suitable humidity and temperature environment [1, 2]. There are many facilities used for cold chains, such as refrigerated containers, refrigerated vehicles and refrigerated warehouses [3]. Due to the low temperature required for chilled food, such as 263.15 K, 255.15 K, and 253.15 K [4, 5], the ice may occur on doors which can cause problems [6]. Thus, it is necessary to anti-ice for the door of refrigerated containers and refrigerated warehouses.

The anti-icing technologies can be classified as mechanical, chemical, and thermal anti-icing techniques [7]. Nowadays, the anti-icing technologies are widely used, and investigated in anti-icing coatings, heating wires and anti-condensation [8-10]. Zhao *et al.* [11] put forward a sandwich structural electric heating coating, and found that the sandwich structural electric heating coating with 2% multi-wall carbon nanotubes could obtain the best electric heating properties. Xue *et al.* [12] designed the superhydrophobic anti-icing coating based on cuttlefish juice which could extend the icing time up to 144 seconds. Zhao *et al.* [13] inves-

* Corresponding authors, e-mail: jfwang@shou.edu.cn, jxie@shou.edu.cn

tigated the electric heating coating. If the electric heating coating was consisted of 8 wt.% multi-wall carbon nanotubes and 1:2 polyurethane/paraffin, the anti-icing properties would be the best. Zhao *et al.* [14] combined electric heating coating and super-hydrophobic coating. This combined coating could reduce the energy consumption for anti-icing by 58%. Omid *et al.* [15] studied a novel heating system whose average system COP was 4.6. Compared with common heating system, the heating efficiency was higher which was 55%. Heymsfield *et al.* [16] designed an anti-ice system based on heating wires and renewable energy. Compared to the de-icing system, this system consumed less energy, and it was not influenced by various weather conditions. Yang *et al.* [17] investigated the heating wires used for refrigerator anti-condensation. It was proposed that the real-time updating of the heating wires could be carried out by the derivation of equations related to dew point temperature, which was more energy efficient than traditional heating wire control methods.

Obviously, in the field of anti-icing, the studies about anti-icing coatings are more, and the research about heating wires needs further more investigated. This paper is devoted to studying the anti-icing performance of the refrigerated container door based on various heating wire forms by CFD. In terms of three heating wire forms, the heat transfer in the refrigerated container wall and the uniformity of air-flow distribution are analyzed. Furthermore, the design processes for heating wires used in different refrigerated containers are summarized. The objective is to improve the anti-icing performance of the refrigerated container with heating wires.

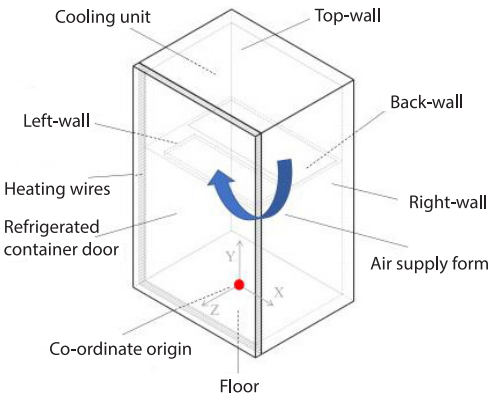

Figure 1. Refrigerated container (3-D view)

Models and methods

Physical model

The model of the researched refrigerated container can be seen in fig. 1. The co-ordinate origin was set on the center of the floor of the refrigerated container. The length of the refrigerated container was 845 mm, the width of refrigerated container was 680 mm, and the height of the refrigerated container was 1325 mm. The thickness of the refrigerated container walls was 40 mm. The materials of refrigerated container walls were vacuum insulation panel (VIP) and polyurethane (PU). The fitted average thermal conductivity was 0.0083 W/mK. In the refrigerated container, there was a cooling unit whose height was 445 mm. The cooling unit covered the entire ceiling of the refrigerated container.

The temperature outside the refrigerated container was 298.95 K. In addition, the initial temperature in the refrigerated container before the operation was also 298.95 K. Moreover, the temperature and air velocity of the supplied wind from the cooling unit were 255.15 K and 1.2 m/s, respectively.

Three heating wire forms were demonstrated in fig. 2. Heating wire form 1 (HWF1), Heating wire form 2 (HWF2), and heating wire form 3 (HWF3) can be seen in figs. 2(b)-2(d). As for HWF1, the used heating wire was adjacent to the external surface of the refrigerated container door wall. As for HWF2, the used heating wire was adjacent to the inner surface of the refrigerated container door wall. As for HWF3, both two heating wires were used at the same time. The material of heating wires is copper. The thermal physical parameters of copper can

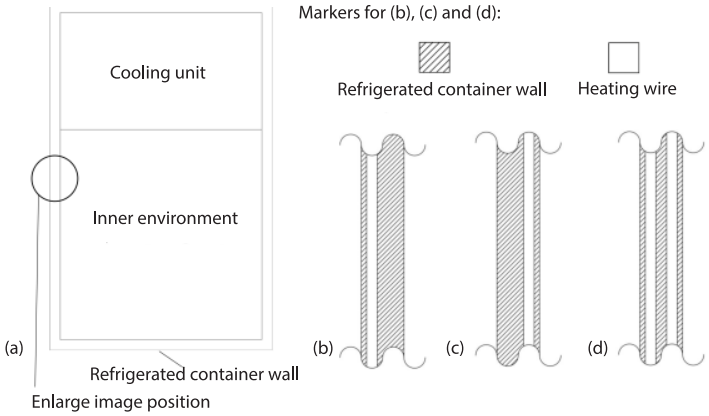

Figure 2. Heating wire forms; (a) enlarge image position for (b)-(d) (front view, cross-section), (b) HWF1 (enlarge image), (c) HWF2 (enlarge image), and (d) HWF3 (enlarge image)

be seen in tab. 1. The power of heating wires was 25 W/m. The diameter of heating wires was 10 mm. The distance between the heating wires and the refrigerated container door was 1 mm. The distance between the heating wires and the nearest surfaces of the refrigerated container were 5 mm.

The models of refrigerated container with HWF1, HWF2, and HWF3 were established by SolidWorks 2014.The tetrahedral meshes of these models were drawn by Workbench 18.0. All values of skewness of these models were below 0.9.

Table 1. Thermal physical parameters of copper

Materials	ρ [kgm^{-3}]	C_p [Jkg^{-1}K^{-1}]	λ [Wm^{-1}K^{-1}]
Copper	8978	381	387.6

Mathematical model

Model assumptions

The assumptions related to the refrigerated container models are as follows [18-22]:

– The flow medium is the incompressible air.
– The impact of solar radiation is neglected.
– The thermal conductivity of refrigerated container wall is fitted by the thermal conductivities of VIP and PU.
– The heating wires are constant temperature heat sources.

Governing equations

The 3-D continuity equations, momentum equations and energy equations are main governing equations [19, 23, 24]:

– The 3-D continuity equation:

$$\frac{\partial \rho}{\partial t} + \vec{\nabla}\left(\rho \vec{\mathrm{v}}\right) = 0 \tag{1}$$

where $\vec{\mathbf{v}}$ [ms^{-1}] is the air velocity, t [s] – the time, and ρ [kgm^{-3}] – the density.

– Momentum equations:

$$\frac{\partial\rho}{\partial t}(\rho v_i)+\frac{\partial\rho}{\partial x_i}(\rho v_i v_j)=\frac{\partial\rho}{\partial x_i}\left[-p\delta_{ij}+\mu\left(\frac{\partial v_i}{\partial x_i}+\left(\frac{\partial v_j}{\partial x_i}\right)\right)\right]+\rho g_i \tag{2}$$

$$\frac{\partial\rho}{\partial t}(\rho v_i)+\frac{\partial\rho}{\partial y_i}(\rho v_i v_j)=\frac{\partial\rho}{\partial y_i}\left[-p\delta_{ij}+\mu\left(\frac{\partial v_i}{\partial y_i}+\left(\frac{\partial v_j}{\partial y_i}\right)\right)\right]+\rho g_i \tag{3}$$

$$\frac{\partial\rho}{\partial t}(\rho v_i)+\frac{\partial\rho}{\partial z_i}(\rho v_i v_j)=\frac{\partial\rho}{\partial z_i}\left[-p\delta_{ij}+\mu\left(\frac{\partial v_i}{\partial z_i}+\left(\frac{\partial v_j}{\partial z_i}\right)\right)\right]+\rho g_i \tag{4}$$

where x, y, and z [m] are the co-ordinate directions, ρ [kgm^{-3}] – the density, p [Pa] – the fluid pressure, g [9.81 ms^{-2}] – the gravity, μ [m^{2}s^{-1}] – the dynamic viscosity, δ – the thick of the wall, the value is 0.04 m, and v [ms^{-1}] – the air velocity.

– Energy equation:

$$\rho\frac{\partial(uT)}{\partial x}+\rho\frac{\partial(vT)}{\partial y}+\rho\frac{\partial(wT)}{\partial z}=\frac{\lambda}{C_p}\left(\frac{\partial^2 T}{\partial x^2}+\frac{\partial^2 T}{\partial xy^2}+\frac{\partial^2 T}{\partial z^2}\right) \tag{5}$$

where u [ms^{-1}] is the air velocity in the x-direction, v [ms^{-1}] – the air velocity in the y-direction, w [ms^{-1}] – the air velocity in the z-direction, λ [WmK] – the thermal conductivity, and T [K] – the temperature.

Boundary conditions

– Inlet boundary

The velocity-inlet boundary was set at the air supply outlet of the cooling unit. In terms of this inlet, the temperature was 255.15 K, and the velocity was 1.2 m/s.

– Outlet boundary

The outflow boundary was set at the return air vent of the cooling unit.

– Wall boundary

The temperature of the external surface of the refrigerated container wall was set as 298.95 K. The thermal conductivity of the refrigerated container wall was set as 0.0083 W/mK.

– Heating wires

The material of heating wires was set as copper. The power of heating wires was set as 25 W/m.

Solution methods

The numerical solution was conducted by Workbench 18.0. The initial temperature in the refrigerated container was 298.95 K. The Fluent transient solver, Pressure-Based solver and the k-ε turbulence model were chosen. The simulated operation time was 3600 seconds. The time step was 100 seconds with 20 iterations. In terms of momentum, energy, turbulent kinetic energy, and turbulent dissipation rate, the First Order Upwind was chosen as the discrete format. The solution of the pressure-velocity coupling was set as SIMPLE.

Grid independence check

As shown in fig. 3(a), the unstructured 3-D mesh was used for this numerical simulation. The maximum skewness was chosen to evaluate the quality of the mesh. The skewness

values for 50000 to 4.9 million meshes are shown in fig. 3(b). After 650000 meshes, the number of meshes did not have a significant effect on the deviation of the meshes. In addition, the skewness of 650000 grids was only 5.22% higher compared to the skewness of 4.9 million grids, and the temperature only varied by 0.0005%. Therefore, the number of 650000 grids was chosen for the numerical calculation in order to reduce the computational effort.

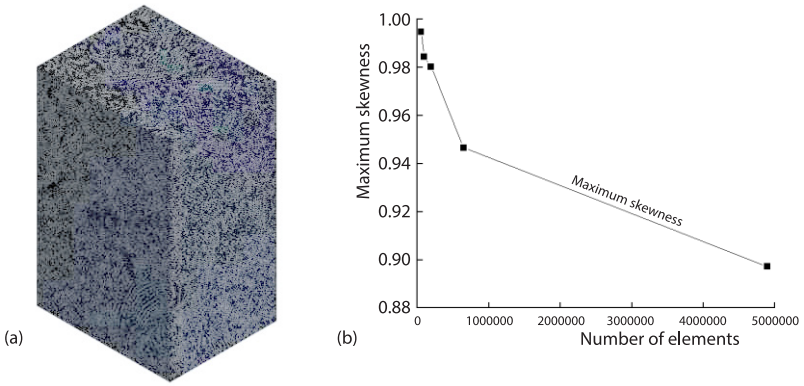

Figure 3. Grid independence; (a) mesh model and (b) max-skewness at different number of elements

Verification

The experiment used to verify the accuracy of models was carried out on the refrigerated container testing bench (RCTB) at HWF3, which was demonstrated in fig. 4(a). The measurement points on the inner surface of the refrigerated container door are shown in fig. 4(b). The operation parameters were the same as those in the numerical simulation, which can be seen in tab. 2. In tab. 3, there were all experimental data and corresponding simulated data. The largest deviation is 0.451%, which is acceptable. Therefore, the models of refrigerated containers are accurate.

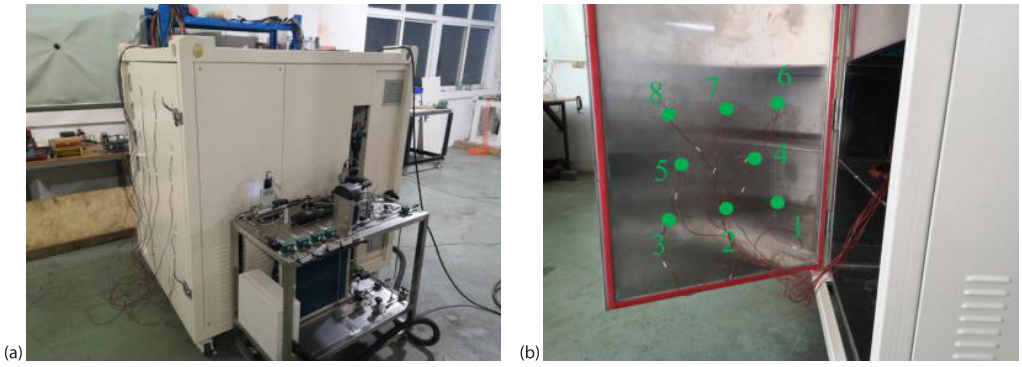

Figure 4. Validation platform; (a) RCTB and (b) arrangement of measurement points

Table 2. Operation parameters

	Ambient temperature [K]	Air supply temperature [K]	Air supply velocity [ms^{-1}]	Operation time [s]
Value	298.95	255.15	1.2	3600

Table 3. Comparison between the experimental data and the simulated data

MP	*ED* [K]	*SD* [K]	*TD* [K]	Deviation
1	255.48	255.492	0.012	0.005%
2	255.17	255.481	0.311	0.122%
3	256.59	255.488	1.102	0.429%
4	255.71	255.441	0.269	0.105%
5	256.03	255.444	0.586	0.229%
6	255.64	255.406	0.234	0.092%
7	255.53	255.412	0.118	0.046%
8	256.57	255.412	1.158	0.451%

Measurement point – MP, experimental data – ED, simulated data – SD, temperature difference – TD

Results and discussions

Heat transfer in the refrigerated container wall

The anti-icing performances of the refrigerated container wall at HWF1, HWF2, and HWF3 are analyzed based on the *X-Y* plane with z = 0.294 m. This plane is a cross-section where the refrigerated container wall, the heating wires and the low temperature environment can be shown simultaneously. When the operation time is 3600 seconds, the heat transfer of the refrigerated container at HWF1, HWF2, and HWF3 are demonstrated in figs. 5(a)-5(c), respectively.

As shown in figs. 5(a) and 5(b), there are two main phenomena in the temperature distribution of refrigerated container door wall. The first phenomenon occurs in the zone between the external environment and the heating wire. In this zone, the temperatures of the refrigerated container door wall at HWF1 and HWF2 are higher, which are higher than 290.19 K. In this zone, there are smaller changes in the temperature gradient. The other phenomenon occurs in the zone between the heating wire and the inner environment. In this zone, the temperatures are lower, but temperature gradient change is more intense. The external environment can be defined as the heat source. The running heating wires are also heat sources. The temperature differences between the two heat sources are smaller. However, the temperature differences between the running heating wire and the inner environment are larger. Thus, the aforementioned trends appear. In terms of the anti-icing performance of the refrigerated container wall, if the temperature of the refrigerated container door wall is larger, the refrigerated container door will be more difficult to be iced. Looking again at figs. 5(a) and 5(b), the temperature of the

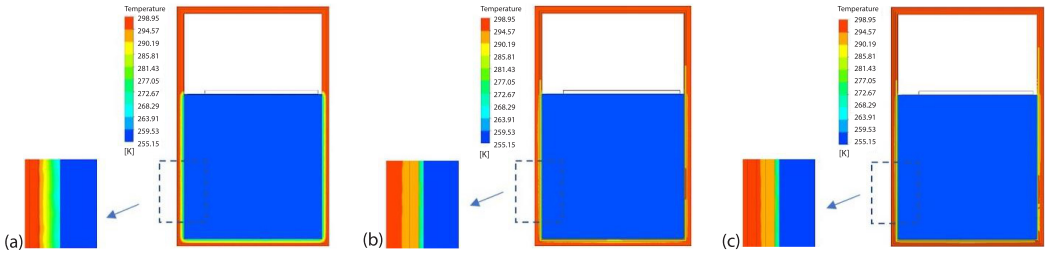

Figure 5. Temperature cloud diagrams of the *X-Y* plane with z = 0.294 m (front view) at the operation time of 3600 seconds, (a) HWF1, (b) HWF2, and (c) HWF3

refrigerated container wall at HWF2 is higher than the temperature of the refrigerated container wall at HWF1 at a location close to the internal environment. Therefore, when the HWF2 is utilized, the anti-icing performance of the refrigerated container door is better. Furthermore, in the comparison of figs. 5(b) and 5(c), the temperature distribution of refrigerated container wall at HWF2 and HWF3 are similar. Thus, when both two heating wires are running, the heating wire more adjacent to the inner environment plays a leading role.

In the design of refrigerated containers, the insulated performance is as important as the anti-icing performance, so it is necessary to analyze the heat flux of the refrigerated container wall [18]. The average heat fluxes on three planes of the left-wall are analyzed. The distance between these three planes and the external surface of the left-wall are 3 mm, 20 mm, and 37 mm, respectively. As shown in fig. 6, the average heat flux of the left wall of HWF1 is higher than that of HWF2 and HWF3 with the same plane, and the average heat flux of the left wall of HWF2 and HWF3 is almost the same. The lower average heat flux means that less heat energy passes through the unit area per unit time and the insulation performance of the refrigerated box wall is better. Therefore, when HWF2 or HWF3 is utilized, the insulation performance of the refrigerated container is better.

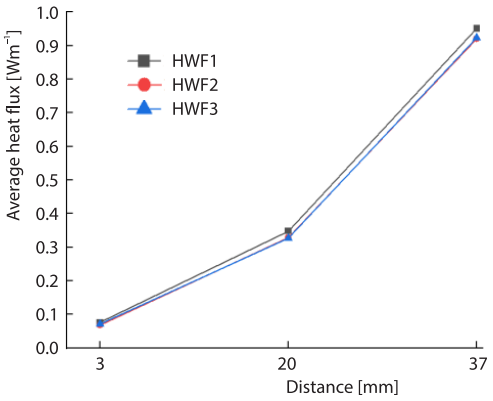

Figure 6. Variation of average heat flux on three planes

In summary, the anti-icing performance and the insulation performance of the refrigerated container door walls of HWF2 and HWF3 are similar. Compared with HWF1, HWF2, and HWF3 have better anti-icing and insulation performance.

Uniformity of air-flow distribution

When the refrigerated container is utilized to store chilled food, the spacings between refrigerated container walls and chilled food can improve the uniformity of air-flow distribution [25]. When the heating wires are running, the low temperature environment adjacent to the refrigerated container door may be influenced by the heat flux from the heating wires. To analyze the impact of uniformity of air-flow distribution with refrigerated container at HWF1, HWF2, and HWF3, the coefficient of velocity non-uniformity (COVN) is calculated [26]. Smaller COVN means the better uniformity of air-flow distribution, which is calculated:

$$COVN = \frac{1}{v_{\text{ave}-t}} \sqrt{\frac{1}{n} \sum_{i=1}^{n} \left(v_{i-t} - v_{\text{ave}-t} \right)^2} \tag{6}$$

where v_{i-t} [ms^{-1}] is the air velocity of each measurement point, $v_{\text{ave}-t}$ [ms^{-1}] – the average air velocity, and n – the quantity of measurement points.

The arrangement of measurement points can be seen in fig. 7(a). There are seven cross-sections chosen in each model. The distances between the inner surface of the refrigerated container door and these cross-sections are 5 mm, 15 mm, 25 mm, 35 mm, 45 mm, 55 mm, and 65 mm. In each cross-section, there are nine measurement points whose location are demonstrated in fig. 7(a).

As shown in fig. 7(b), when the operation time is 3600 seconds, the trends of $COVN_{HWF1}$ curve and $COVN_{HWF2}$ curve are decreasing with the increase of the distance between the inner surface of refrigerated container door and the cross-section. Thus, when there is one heating wire used, if the chilled food is placed farther away from the refrigerated container wall, the uniformity of air-flow distribution will be better. On the same cross-section, the values of COVN from largest to smallest are $COVN_{HWF3}$, $COVN_{HWF1}$, and $COVN_{HWF2}$, respectively, the decline rates of COVN from largest to smallest are $COVN_{HWF2}$, $COVN_{HWF1}$, and $COVN_{HWF3}$, respectively. If the value of COVN is smaller and the decline rate of COVN is larger, the more uniform air-flow distribution will be achieved. The first result is that using one heating wire can obtain better uniformity of air-flow distribution than using two heating wires. The other result is that if the heating wire is more adjacent to the inner environment of the refrigerated container, the uniformity of air-flow distribution will be better.

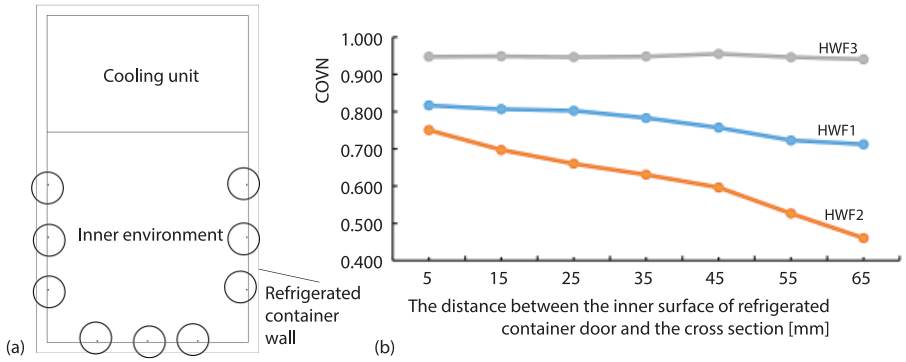

Figure 7. The variation of COVN curves at the operation of 3600 seconds; (a) arrangement of measurement points on each cross-section (front cutaway view) and (b) COVN curves

In summary, when the HWF2 is utilized, the best uniformity of air-flow distribution can be obtained.

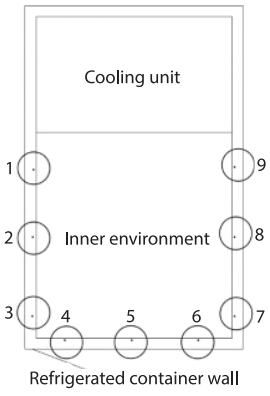

Figure 8. Arrangement of measurement points on each cross-section (front cutaway view)

Coefficient of thermal conductivity

The thermal conductivity of the refrigerated container wall plays an important role in anti-icing. As the thermal conductivity increases, the temperature of the fluid domain has a greater effect on the refrigerated container door. Therefore, it is necessary to study the effect of HWF1, HWF2, and HWF3 on the anti-freezing performance of the refrigerated box wall when the thermal conductivity is different. As shown in fig. 8, nine points are taken on the door of the box near the inner wall surface, and the co-ordinates of these nine points are shown in tab. 4. As shown in figs. 9(a)-9(c), the temperature on the refrigerator door decreases as the thermal conductivity increases. In fig. 9(a) when the thermal conductivity is below 0.006 W/mK, the use of HWF1 causes the freezer door to freeze. However, for using HWF2 and HWF3, when the thermal conductivity reaches 0.01 W/mK, the temperature at all nine points is above 273 K, which means that the freezer door does not freeze. Thus

HWF2 and HWF3 can be used in a larger range than HWF1, with less restriction on the required thermal conductivity of the freezer walls. It can be found by figs. 9(b)-9(c) that the temperature peaks occur near the two corners of the bottom of the refrigerator. So in practice, when the goods need to be placed near the door of the refrigerated container, they should be placed in the middle of the refrigerated container.

Table 4. The co-ordinates of the nine points

Co-ordinate	*X* [mm]	*Y* [mm]	*Z* [mm]
1	38	665	302
2	38	430	302
3	38	220	302
4	200	38	302
5	423	38	302
6	600	38	302
7	807	220	302
8	807	430	302
9	807	665	302

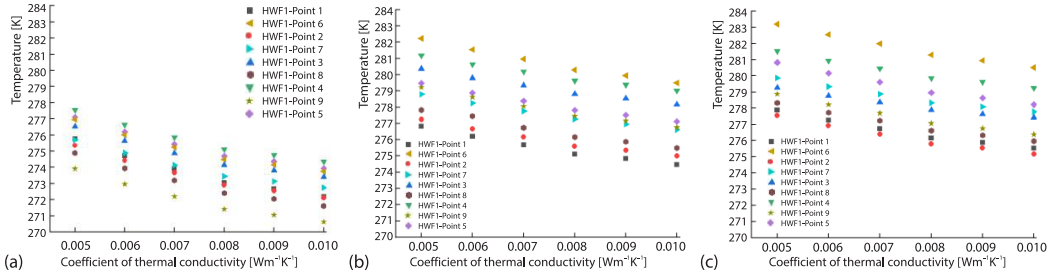

Figure 9. Temperature of nine points with different thermal conductivity; (a) HFW1, (b) HWF2, and (c) HWF3

To sum up, HWF2 and HWF3 can be used in a wider range of thermal conductivity for the wall of the refrigerated container than HWF1. There are less restrictions on materials in actual production.

Design processes for heating wires used in different refrigerated containers

The anti-icing performance of the refrigerated container doors will be good if the electric heating wire is used. When HWF2 and HFW3 are used, better anti-icing performance and better uniformity of air-flow distribution can be obtained. The design solutions of electric heating wires based on the refrigerated container wall thickness can be divided into three types. The installation, operation, and maintenance of electric heating wires can lead to carbon emissions [27], and the more electric heating wires installed or operated, the greater the carbon emissions. Therefore, it is necessary to install as few electric heating wires as possible. In this study, the width of each electric heating wire is 10 mm.

When the wall thickness of the refrigerated container (WTRC) is less than 50 mm, an electric heating wire should be placed at the surface of the inner wall. When 50 mm $\leq$ WTRC $\leq$ 90 mm, two electric heating wires should be installed on the wall of the refrigerated

container. The two electric heating wires are evenly distributed within the inner wall surface. The electric heating wire near the inner wall surface is the main electric heating wire used for anti-icing. The other heater wire is the backup wire used to maintain the anti-icing performance when the main heater wire is damaged. When WTRC is greater than 90 mm, there are two design options. The design solutions can be divided into two further design solutions.

Two further design solutions are:

– Design solution with three heating wires

This design solution is to evenly install three heating wires in the refrigerated container wall. The heating wire nearest the inner wall surface is the anti-icing wire, and other two heating wires are spare heating wire. If the heating wire nearest the inner wall surface is damaged, it is necessary to select the middle heating wire to the anti-icing heating wire, because the heat transfer distance of the middle heating wire is the shortest.

– Design solution with two heating wires

This design solution is to install the heating wire nearest the inner wall surface and the middle heating wire, which can decrease the carbon emission of the anti-icing process in the refrigerated container. If the heating wire nearest the inner wall surface is damaged, another heating wire is selected as the anti-icing heating wire.

According to the different thickness of the refrigerated container wall, there are different design solutions for anti-icing arrangements of electric heating wires. When WTRC < 50 mm, one electric heating wires is selected to place at the nearest to the inner wall surface. When 50 mm ≤ WTRC ≤ 90 mm, two electric heating wires are placed in the refrigerated container door, the first one is placed at the nearest to the inner wall surface, and the second one is placed in the middle of the refrigerated container wall. When WTRC > 90 mm, there can be two design solutions: two or three electric heating wires can be choosed for anti-icing. The electric heating wires nearest to the inner wall surface is the optimal anti-icing solution. When the electric heating wires nearest to the inner wall surface cannot work, the other electric heating wires would be a replacement for it.

Conclusions

In this paper, an anti-icing study of refrigerated containers based on three forms of heating wires was conducted. The heat transfer and thermal conductivity of the refrigerated container wall, and the uniformity of air-flow distribution in the refrigerated container were analyzed. The main conclusions are as follows.

- Compared with HWF1, HWF2, and HWF3 have better anti-icing performance and insulation performance. Compared with HWF3, HWF2 has the better uniformity of air-flow distribution in the refrigerated container. Therefore, HWF2 is the best heating wire form for the anti-icing performance of the refrigerated container.
- When the thermal conductivity is in the range from 0.005-0.01 W/mK, HWF1 has icing at 0.006 W/mK, while HWF2 and HWF3 have the anti-icing situation in the whole range. Therefore, HWF2 and HWF3 are suitable for a wider range of refrigerator door thermal conductivity.
- The electric heating wires nearest to the inner wall surface is the optimal anti-icing solution. When the electric heating wires nearest to the inner wall surface is damaged, the other electric heating wires would be a replacement for it. When 50 mm ≤ WTRC ≤ 90 mm, one spare electric heating wire is placed in the refrigerated container door. When WTRC > 90 mm, one or two spare electric heating wire is placed in the refrigerated container door.

In the future, the anti-icing solution of electric heating wires can be further determined in combination with carbon emission analysis.

Acknowledgment

This research was supported by Science and Technology Innovation Action Plan of Shanghai Science and Technology Commission (19DZ1207503), Public Service Platform Project of Shanghai Science and Technology Commission (20DZ2292200).

Nomenclature

C_p – specific heat capacity, [Jkg^{-1}K^{-1}]
g – gravitational acceleration, [9.8 ms^{-2}]
n – quantity of measurement points, [–]
p – fluid pressure, [Pa]
T – temperature, [K]
t – time, [s]
u – air velocity in the x-direction, [ms^{-1}]
v – air velocity in the y-direction, [ms^{-1}]
v_{ave-t} – average air velocity, [ms^{-1}]
v_{i-t} – air velocity of each measurement point, [ms^{-1}]
$\vec{\mathbf{v}}$ – air velocity, [ms^{-1}]
w – the air velocity in the z-direction, [ms^{-1}]
x – x-co-ordinate, [m]
y – y-co-ordinate, [m]
z – z-co-ordinate, [m]

Greek symbols

δ – thickness of the wall, [m] (0.04 m)
λ – thermal conductivity [Wm^{-1}K^{-1}]
μ – dynamic viscosity [m^{2}s^{-1}]
ρ – density [kgm^{-3}]

Acronyms

COVN – coefficient of velocity non-uniformity
PU – polyurethane
RCTB – refrigerated container testing bench
VIP – vacuum insulation panel
WTRC – the wall thickness of the refrigerated container
HWF1 – heating wire form 1
HWF2 – heating wire form 2
HWF3 – heating wire form 3

References

[1] Liu, E. H., *et al*., Fractal Calculus for Refrigerated Transportation of Perishable Foods Energy Consumption and Energy Saving, *Thermal Science*, *25* (2021), 2B, pp. 1255-1260
[2] Devireddy, R. V., Biopreservation: Heat/Mass Transfer Challenges and Biochemical/Genetic Adaptations In Biological Systems, *Heat Transfer Research*., *44* (2013), 3-4, pp. 245-272
[3] Yang, F. Y., *et al*., Research on Quasi-Two-Stage compression cycle characteristics of referigeration system for cold storage, *Thermal Science*, *26* (2022), 3B, pp. 2765-2770
[4] Wang, J. F., *et al*., Effect of Glazing with Different Materials on the Quality of Tuna during Frozen Storage, *Foods*, *9* (2020), 231
[5] Tan, M. T., *et al.*, Storage Time Prediction of Glazed Frozen Squids during Frozen Storage at Different Temperatures Based on Neural Network, *International Journal of Food Properties*, *23* (2020), *1*, pp. 1663-1677
[6] Ibrahim, Y., *et al*., The 3-D Printed Electro-Thermal anti- or de-Icing System for Composite Panels, *Cold Regions Science and Technology*, *166* (2019), 102844
[7] Nilsson, F., *et al*., Modelling Anti-Icing of Railway Overhead Catenary Wires by Resistive Heating, *International Journal of Heat and Mass Transfer*, *143* (2019), 118505
[8] Redondo, O., *et al*., Anti-Icing and De-icing Coatings Based Joule's Heating of Graphene Nanoplatelets, *Composites Science and Technology*, *164* (2018), Aug., pp. 65-73
[9] Voigt, A. L., *et al*., Conception, Implementation and Evaluation of Induction Wire Heating System Applied to Hot Wire GTAW (IHW-GTAW), *Journal of Materials Processing Tech*., *281* (2020), 116615
[10] Li, J., *et al*., Study on Optimization of Condensation Prevention and Power Consumption of Refrigerator Glass Door, *Proceedings*, China Household Appliance Technology Conference, China, 2019, pp. 339-350
[11] Zhao, Z. H., *et al*., Novel Sandwich Structural Electric Heating Coating for anti-Icing/de-Icing on Complex Surfaces, *Surface and Coatings Technology*, *404* (2020), 126489
[12] Xue, C. H., *et al*., Superhydrophobic anti-Icing Coatings with Self-Deicing Property Using Melanin Nanoparticles from Cuttlefish Juice, *Chemical Engineering Journal*, *424* (2021), 130553
[13] Zhao, Z. H., *et al*., The Development of Electric Heating Coating with Temperature Controlling Capability for anti-Icing/de-Icing, *Cold Regions Science and Technology*, *184* (2021), 103234
[14] Zhao, Z. H., *et al*., Development of High-Efficient Synthetic Electric Heating Coating for anti-icing/de-Icing, *Surface and Coatings Technology*, *349* (2018), Sept., pp. 340-346
[15] Omid, H. B., *et al*., A Novel Full-Scale External Geothermal Heating System for Bridge Deck de-Icing, *Applied Thermal Engineerin*g, *185* (2021), 116365

[16] Heymsfied, E., *et al*., Developing anti-Icing Airfield Runways Using Surface Embedded Heat Wires and Renewable Energy, *Sustainable Cities and Society*, *52* (2020), 101712
[17] Yang, Z. H., *et al*., Energy-Saving Optimization of Anti-condensation Heating Wire for Refrigerator, *Proceedings*, 2019 China Household Appliance Technology Conference, China, 2019, pp. 246-250
[18] Gaedtke, M., *et al*., Application of a Lattice Boltzmann Method Combined with a Smagorinsky Turbulence Model to Satially Resolved Heat Flux Inside a Refrigerated Vehicle, *Comput. Math. Appl.*, *76* (2018), 10, pp. 2315-2329
[19] Jara, P. B. T., *et al*., Thermal Behavior of a Refrigerated Vehicle: Process Simulation, *Int. J.Refrig*., *100* (2018), Apr., pp. 124-130
[20] Nikitin, M. N., Numerical Analysis of Refrigerated Display Designs in Terms of Cooling Efficiency, *Int. J. Therm. Sci*., *148* (2020), 106157
[21] Radwan, A., *et al*., Thermal and Electrical Performances of Semi-Transparent Photovoltaic Glazing Integrated with Translucent Vacuum Insulation Panel and Vacuum Glazing, *Energ. Convers. Manage*., *215* (2020), 112920
[22] Li, W., Simulation and Experimental Study on Temperature Field of Refrigerator Against Condensation, *Journal of Appliance Science and Technology*, *02* (2021), 2, pp. 104-110
[23] Han, J.W., et al., Computational Fluid Dynamics Simulation Determine Combined Mode to Conserve Energy in Refrigerated Vehicles, *Journal Food Process Eng*., *39* (2016), 2, pp. 186-195
[24] Li, J., *et al.*, Effect of Coverage Percentage of Vacuum Insulation Panels on Inner Temperature Distribution of Refrigerated Container, *Food and Machinery*, *32* (2016), 07, pp. 99-102+165
[25] Guo, J. M., *et al*., Numerical Simulation on Temperature Field Effect of Stack Method of Garden Stuff for Fresh-Keeping Transportation, *Transactions of the Chinese Society for Agricultural Engineering*, *28* (2012), 13, pp. 231-236
[26] Liu, X. F., Nan, X. H., Improvement on Characteristics of Air-Flow Field in Cold Storage with Uniform Air Supply Duct, *Transactions of the Chinese Society of Agricultural Engineering*, *32* (2016), 01, pp. 91-96
[27] Xu, H. P., *et al*., Carbon Emission Analysis of Passive Timber Buildings in Severe Cold Region Based on Type Comparison, *Architecture Technology*, *52* (2021), 3, pp. 324-328

Paper submitted: October 13, 2022
Paper revised: November 25, 2022
Paper accepted: November 28, 2022